FINAL VERSION OF PAPER REFERENCE: H/PI.37

MESOSCOPIC MODELLING OF ENAMEL INTERACTION WITH MID-INFRARED SUB-ABLATIVE LASER PULSES

A. Vila Verde[1], Marta M. D. Ramos[1**], R. Mendes Ribeiro[1] and Marshall Stoneham[2]

[1] Department of Physics, University of Minho, Campus de Gualtar, 4710-057 BRAGA, PORTUGAL

[2]Department of Physics and Astronomy, University College London, Gower Street, London WC1E 6BT, United Kingdom

---

Abstract

Using a Finite Element approach the authors model the influence of enamel's microstructure and water distribution on the temperature and stress at the centre of the laser spot, for a CO_2 laser working at 10.6 μm, with 0.35 μs pulse duration and sub-ablative

* Corresponding Author: Tel. +351 253 604 320; Fax. +351 253 678 981; E-mail: marta@fisica.uminho.pt
Departamento de Física, Universidade do Minho, Campus de Gualtar, 4710-057 BRAGA, PORTUGAL

intensity. The authors found that the distribution of water in enamel significantly influences the stress generated at the end of one laser pulse: much lower (two orders of magnitude) stress values occur in models with homogeneously distributed water than in models with 0.27% vol. water located in pores or 4% vol. in layers. The amount of water in enamel has a strong influence on the stress distribution, but not on the maximum stress values reached. On the other hand, different water contents do not influence the temperature distribution in enamel

These results suggest that adequate modelling of the ablation mechanisms in enamel, as in other highly inhomogeneous materials, must include their structure at the mesoscopic scale.

Keywords: mesoscopic modelling; laser ablation; enamel; finite element method; CO_2 laser

---

1. Introduction

The capability of lasers for precisely ablating and machining materials and living tissues is already established. Although lasers are already used, even commercially, for this purpose, these procedures are not necessarily optimised for all materials and lasers: sufficient precision and predictability of cut may not be available, unwanted thermal or mechanical damage may occur, or it may just be that the speed of the process or its efficiency are below what would be desired. For years there has been specific investigation of the mechanisms involved in laser ablation; however, models with sufficient predictive capability to determine the laser parameters which will optimize ablation procedures do not exist yet [1, 2]. For highly inhomogeneous materials, these models will necessarily have to explicitly consider the microstructure of the material. [3, 4].

The ablation of dental enamel by IR lasers is one of such procedures that is already a reality but is still not optimized. The authors are developing a new mesoscopic modelling capability for this procedure – using Finite Element Analysis - with the aim of contributing for its optimization. Since the role of enamel's micrometer-scale structure, water content and water distribution on dental laser ablation is not known, the authors present their effects on the temperature and stress generated by one sub-ablative laser pulse. Although the mesoscopic structure and material properties involved in the work presented here are specific of dental enamel, the approach being developed by the authors is appropriate to build mesoscopic models of the ablation by IR lasers of highly inhomogeneous materials - such as living tissues or composites with a micrometer-scale structure - in a way which, to the best of our knowledge, has not been done yet.

2. Model description

The authors used Algor^{TM} (commercial finite element software) to create the geometric model of enamel and to obtain its temperature and stress distribution at the end of one laser pulse.

Human dental enamel is composed mainly of carbonated hydroxyapatite and a small percentage of water. To the best of our knowledge, an accurate description of the distribution of water in this tissue is not available in the literature. It is known that more water exists at the boundary of the rods than on their inside, but the exact fraction of water in enamel, the pore size distribution and connectivity are not known [5,6]. Based on this information the authors developed four models of enamel, which differ only on their water content and distribution.

Only a brief description of the models and of the simulation procedure will be presented here. The details can be found elsewhere [7]. The basic enamel rod model can be seen on Fig. 1. Its shape resembles human dental enamel rods. This structure was repeated in order to create 4 larger models, which represent a portion of enamel with dimensions 23 μm × 23 μm × 35 μm: the homogeneously distributed water model, in which all the water is distributed homogeneously at a sub-micrometer scale; the continuous water-layer model, with 4% vol. water forming a continuous layer (all the elements in dark grey in Fig. 1) around each enamel rod; the scattered pores model, with 0.27% vol. water in macropores evenly distributed at the edge of the rod (dark grey region in Fig. 1) and the clustered pores model, also with 0.27% vol. water in macropores that form clusters at the edge of the rod. The homogeneously distributed water model is not representative of enamel, as it is known that its water content is not homogeneously distributed at the micrometer scale [5]. Comparison of the results obtained for the other models with this model allows us to assess the influence of enamel's water content and distribution on the temperature and stress reached at the end of one laser pulse.

The initial temperature of the nodes was 37 ºC. The physical properties assigned to the materials are given in Table 1. The absorption coefficients of hydroxyapatite (HA) and water were considered to be the same and were given the value found in ref. [8] (825 cm^{-1}) for human dental enamel. They are not considered to be a function of temperature, which is a very good approximation for water [9]; although no information was available in the literature regarding HA, the authors adopt the same approximation for this material. The thermal expansion coefficient of water was estimated based on the specific volume of this substance at 293.15 ºK and 373.15 ºK found in ref. [10].

The mechanical properties of the materials were estimated. The mechanical properties of some of the elements at the edges of the geometric model are different from those listed in

table 1, so that appropriate boundary conditions can be established. A detailed description of these estimates can be found in [7]. We considered that all the incident radiation was absorbed and transformed into internal kinetic energy of the material. The optical axis of the laser beam is perpendicular to the surface of the model. The intensity of the laser beam inside the tissue at every instant is given by:

$$I(r,z) = I_0.\exp(-\alpha.z).\exp\left(-\frac{2r^2}{w^2}\right) \quad (1)$$

where r is the distance from the centre of the laser beam, z is the depth inside the tissue, I_0 is the intensity of radiation at the centre of the laser spot, α is the absorption coefficient of the tissue and w is the beam radius [11]. As a result, the laser intensity has a Gaussian profile along r, which decays exponentially along z and it is constant time. The laser parameters used in the simulations are given in Table 2. The fluence used, 0.42 J/cm^2, is below the threshold for laser induced changes on the surface (2-3 J/cm^2 for a pulse with 2 μsec, [12]).

The authors performed transient heat transfer analyses with time-steps of 0.0125 μs duration. The temperature distribution at the end of step 0.35 μs was used as input for the linear static stress analyses.

3. Results and discussion

The temperature distribution at the end of the laser pulse is identical for all studied models. The maximum temperature reached was approximately 160 ºC. The only appreciable

temperature gradients occurred along OZ, that is, parallel to the optical axis of the laser beam. The temperature maps obtained are similar to that published in ref. [7].

The equivalent Von Mises stress for the outer elements of a single enamel rod located at the centre of the non-homogeneous water distributed models is presented in Fig. 2. The equivalent Von Mises stress is a scalar value, calculated from the stress tensor components, which can be compared with the stress values at which a material fails in tension and in compression - ultimate tensile and compressive stress. A maximum Von Mises stress of 2 GPa is reached in all models presented in Fig.2. The maximum Von Mises stress for the homogeneously distributed water model (figure not presented) is 2 orders of magnitude lower. These results seem to indicate that the maximum Von Mises stress does not depend on the amount of water but it depends on water distribution within enamel. The pores models have very similar distributions of Von Mises stress, but very different from that observed on the water-layer model. However, the three models have one common characteristic: higher stress values are associated with regions with higher water content. The Von Mises stress map for the homogeneously distributed water model is qualitatively and quantitatively different from the ones presented in Fig. 2. The results discussed above indicate that the presence of as little as 0.27 % vol. water in macropores in enamel can have a drastic influence on the mechanical response of this material to the absorption of radiation.

The ZZ component of the stress tensor for the non-homogeneous water distributed models is presented in Fig. 3. Its intensity throughout the structure is dependent on the amount of water and its distribution. In the continuous water-layer model, the elements located at the tail of the rods experience the highest values of tensile stress along OZ. This consideration suggests that ablation should start in this region if this water distribution is representative of enamel. In the pores models, the elements located at a large inner part of the structure (visible in Fig. 3b) experience the highest tensile ZZ stress values. This fact does not seem to be

related to the material distribution, since a similar stress distribution occurs in the homogeneously distributed water model. The ZZ stress maps obtained for the clustered and scattered pores models are similar: the pores experience higher compressive ZZ stress values. However, this situation may not occur at higher laser intensities, when water vaporization occurs. The maximum ZZ tensile stress component for the clustered pores model is approximately double than for the scattered pores model, which suggests that the geometry of the macropore distribution may have some influence on the relative intensity of the stress tensor components. The differences found for the stress component along the material-removal direction can have a marked influence on the ablation process.

4. Conclusions

The preliminary results presented indicate that the mechanical response of enamel when as little as 0.27 % vol. water is located in macropores is significantly different from the homogeneous distribution. These results suggest that, in order to adequately describe the mechanisms of ablation in enamel by CO_2 lasers, the material's structure at the micrometer scale must be included, which indicates that explosive material removal caused by pressure build up in water-rich regions may play an important role during ablation of enamel.

From a more general point of view, these results suggest that, in order to better understand the ablation mechanisms of composite materials with a micrometer-scale structure, a mesoscopic approach should be taken. A description of the ablation mechanisms assuming the material does not have structure or variable chemical composition will provide important information by itself, but may be incomplete and perhaps misleading.

5. Acknowledgements

This work was approved by the Portuguese Foundation for Science and Technology and supported by the European Community Fund FEDER under project no. POCTI/ESP/37944/2001. One of us (A.V.V.) is also indebted to FCT for financial support under PhD grant no. SFRH/BD/4725/2001. The authors wish to thank Drs. G. Dias and J. Carneiro, from the University of Minho, and Profs. G. Pearson and J. Elliot from Queen Mary Westfield College, London, for helpful discussions in the course of this work.

References

[1] G. Paltauf, P.E. Dyer, Chemical Reviews 103 (2003) 487.

[2] A. Vogel, V. Venugopalan, Chemical Reviews 103 (2003) 577.

[3] A.M. Stoneham, J.H. Harding, Nature Materials 2 (2003) 77.

[4] A.M. Stoneham, M.M.D. Ramos, R.M. Ribeiro, Applied Physics A 69 (1999) s81.

[5] J.C. Elliott, F.S.L. Wong, P. Anderson, G.R. Davis, S.E.P. Dowker, Connective Tissue Research 39 (1998) 61.

[6] G.H. Dibdin, Car. Res. 27 (1993) 81.

[7] A. Vila Verde, M.M.D. Ramos, R.M. Ribeiro, A.M. Stoneham, Proc. of SPIE Vol. 4950 Lasers in Dentistry IX (2003) 72.

[8] M.J. Zuerlein, D. Fried, J.D.B. Featherstone, W. Seka, Ieee Journal of Selected Topics in Quantum Electronics 5 (1999) 1083.

[9] R.K. Shori, A.A. Walston, O.M. Stafsudd, D. Fried, J.T. Walsh, Ieee Journal of Selected Topics in Quantum Electronics 7 (2001) 959.

[10] J.R. Cooper, E.J. Le Fevre, Thermophysical properties of water substance - Student's tables in SI units, Edward Arnold Ltd, London, 1975.

[11] H. Markolf Niemz, Laser-Tissue Interactions, Springer-Verlag, Berlin,1996.

[12] D. Fried, J. Ragadio, M. Akrivou, J. Featherstone, M.W. Murray, K.M. Dickenson, Journal of Biomedical Optics 6 (2001) 231.

[13] H.H. Moroi, K. Okimoto, R. Moroi, Y. Terada, International Journal of Prosthodontics 6 (1993) 564, in "Dental Tables" at http://www.lib.umich.edu/.

[14] D. Bloor, M.C. Flemings, R. Brook, S. Mahajan, R. Cahn,(Eds.), The encyclopedia of advanced materials, vol. 4, Elsevier Science Ltd, Great Britain, 1994, pp. 1076.

List of Graphics Captions

Fig. 1. a) Cross-sectional view of enamel rod. b) Side-view of enamel rod. The dark area corresponds to the water/organic matrix, and the light area to the HA core. The thinner area is termed the tail or waist while the wider area is commonly described as the head of the rod.

Fig. 2. Equivalent Von Mises stress (N/m^2) for the outer elements - correspond to the darker areas visible in Fig. 1. - of a single enamel rod a) Continuous layer model. b) Scattered pores model. c) Clustered pores model.

Fig. 3. ZZ ccomponent of stress (N/m^2). In each finite element, a positive value of stress indicates that it is under tension along OZ; a negative value indicates that that element is being compressed along OZ. The models were sectioned in half so that we could observe the stress distribution inside. a) Continuous layer model. b) Scattered pores model. c) Clustered pores model.

Table 1
Material parameters used in simulations. The elements at the lower part of the models act as a heat sink* and also simulate the more flexible dentine which lies beneath enamel [#].

.

	Water	Mineral	Elements at the lower part of the models
Absorption coefficient (cm^{-1})	825	825	0
Thermal conductivity (J/(s.m.ºC))	0.6 [10]	1.3 [13]	0
Specific heat (J/(kg.ºC))	4.2×10^3	8.8×10^2 [13]	8.8×10^2
Mass density (kg/m^3)	1×10^3	3×10^3 [5]	$^{*}\ 3 \times 10^6$
Young's modulus (N/m^2)	1.9×10^{10}	1.1×10^{11}	$^{\#}\ 1.5 \times 10^6$
Poisson's ratio	0.28	0.28	0.28
Thermal expansion coefficient ($ºC^{-1}$)	5×10^{-4}	1.6×10^{-5} [14]	0

Table 2

Laser parameters

Type of laser	CO_2 at 10.6 μm
Pulse duration (μs)	0.35
Intensity, I_0 ($J/(m^2.s)$)	1.2×10^{10}
Number of pulses	1
Beam waist (mm)	0.2

Fig. 1 a)

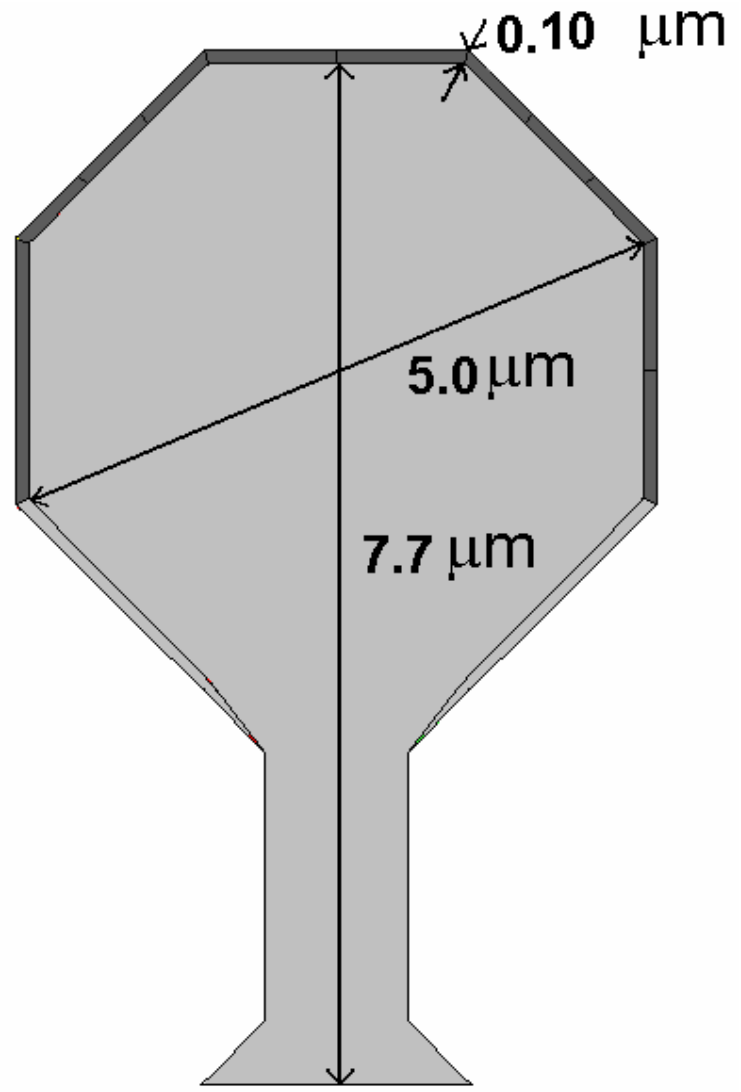

Fig. 1 b)

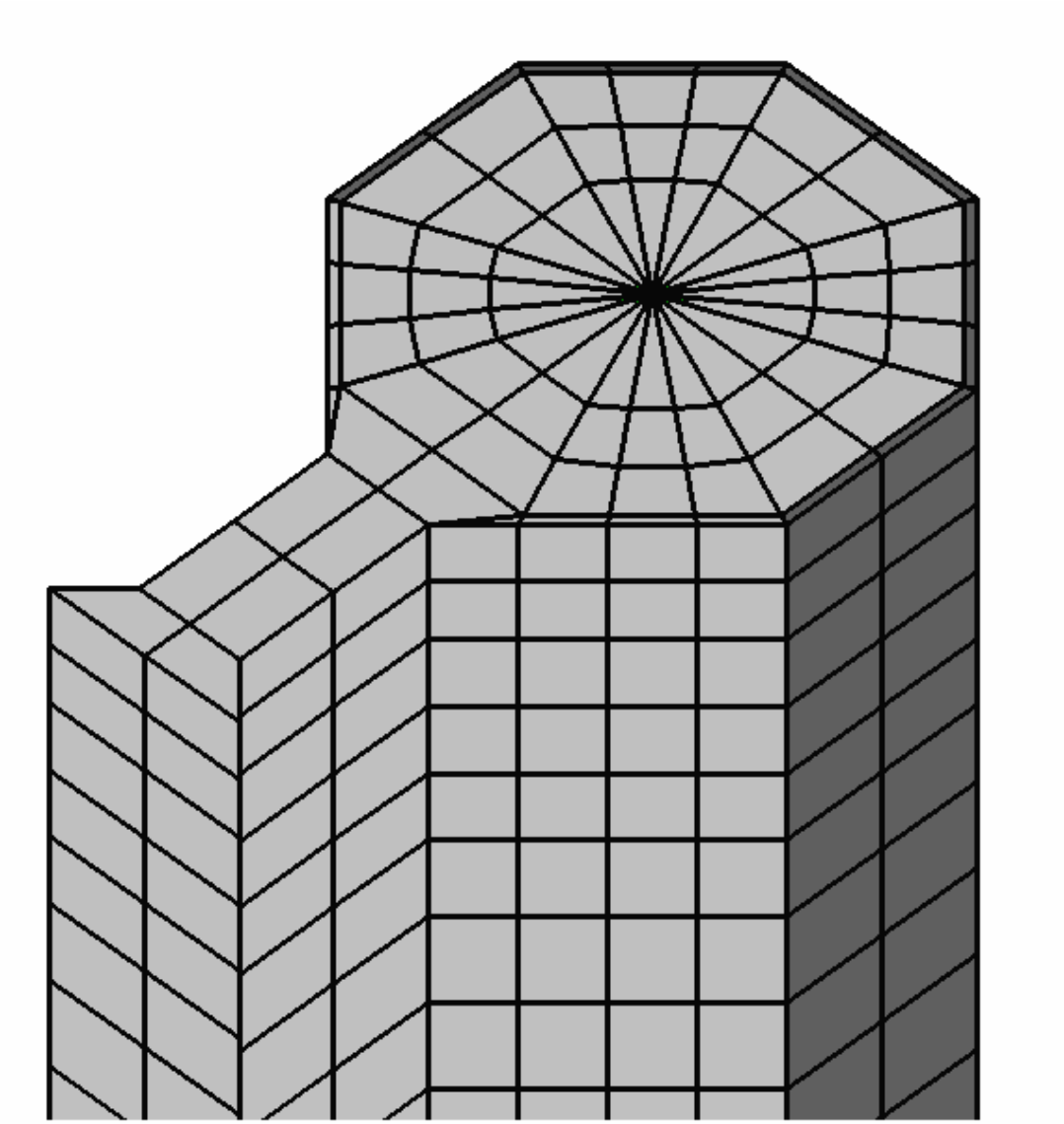

Fig. 2a

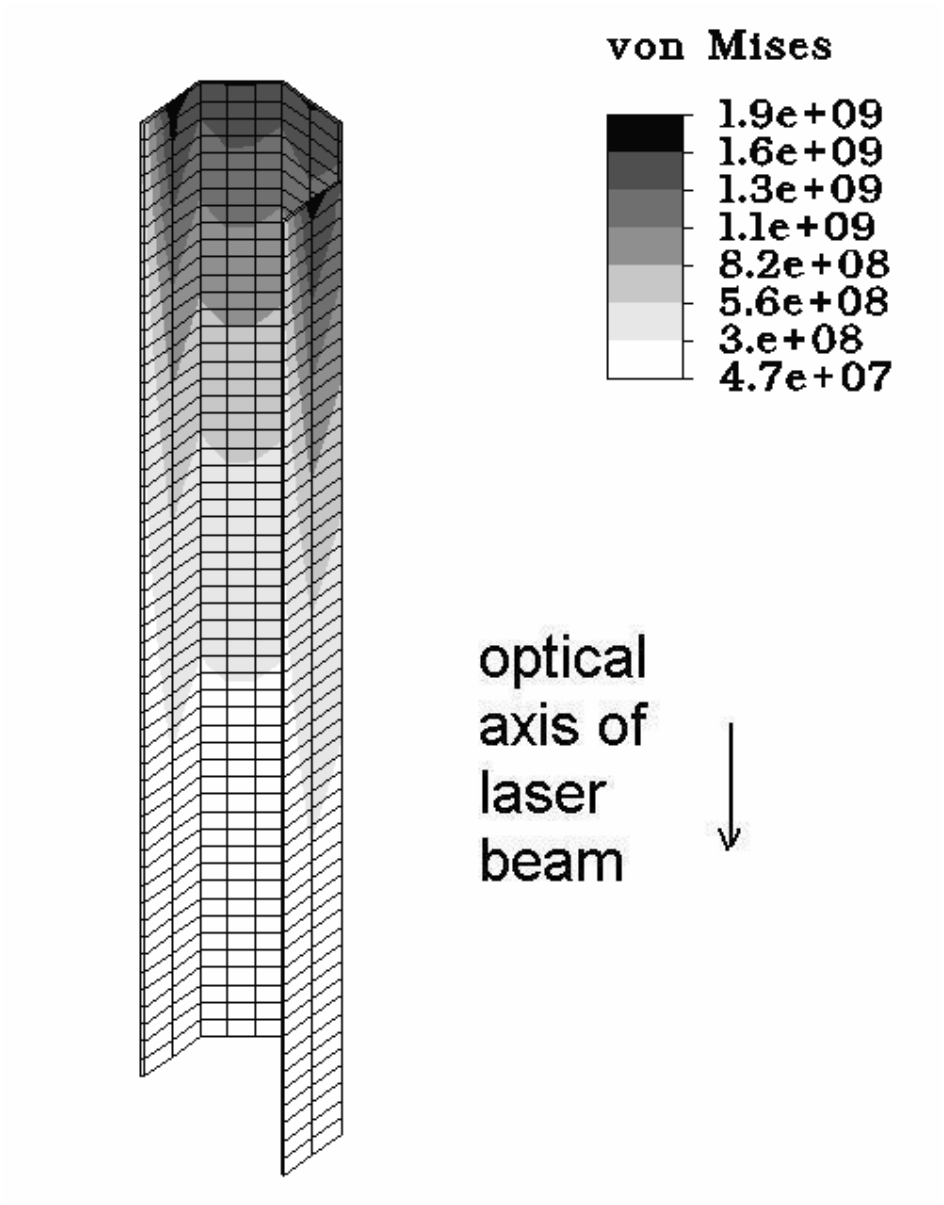
von Mises
1.9e+09
1.6e+09
1.3e+09
1.1e+09
8.2e+08
5.6e+08
3.e+08
4.7e+07
optical
axis of
laser
beam

Fig. 2b

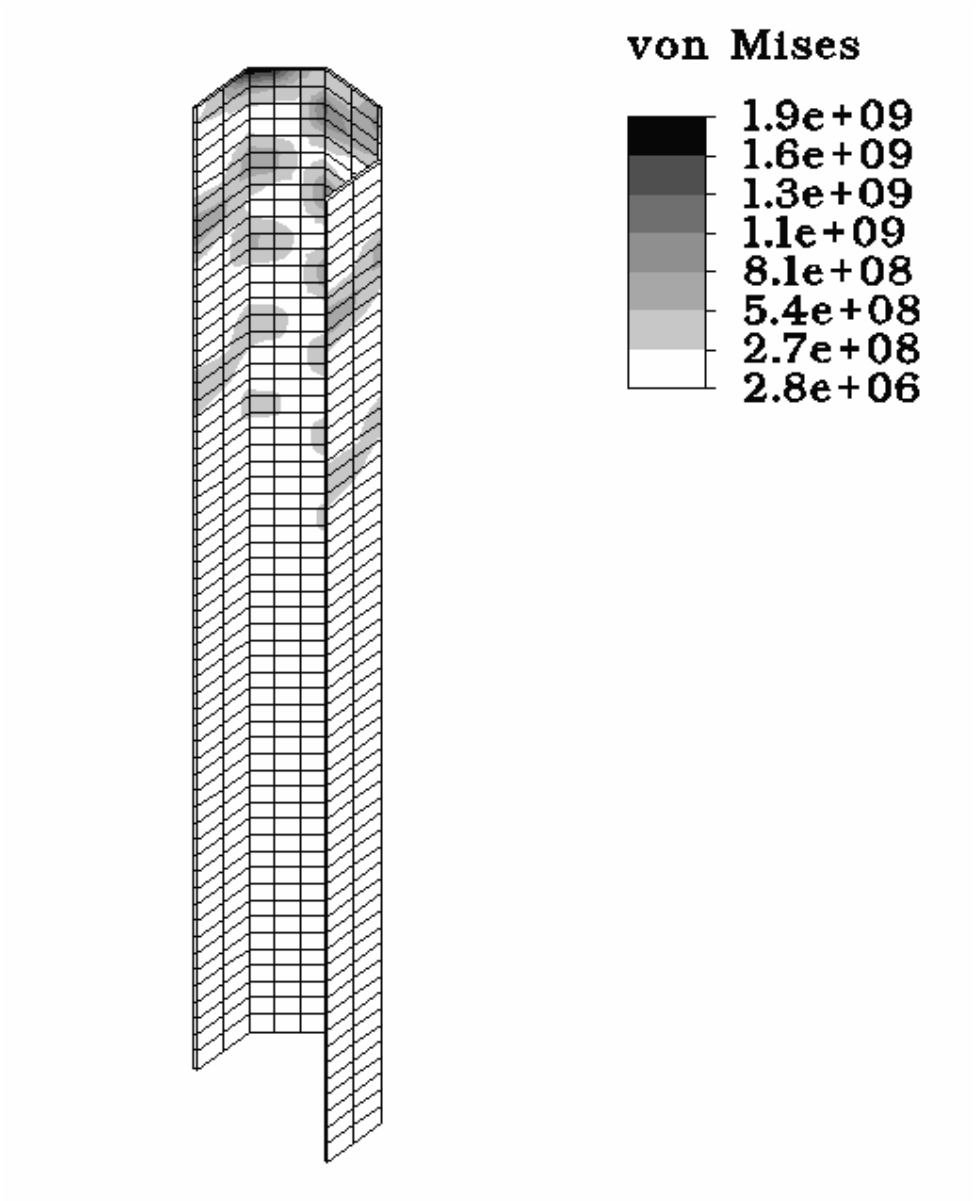

Fig. 2c

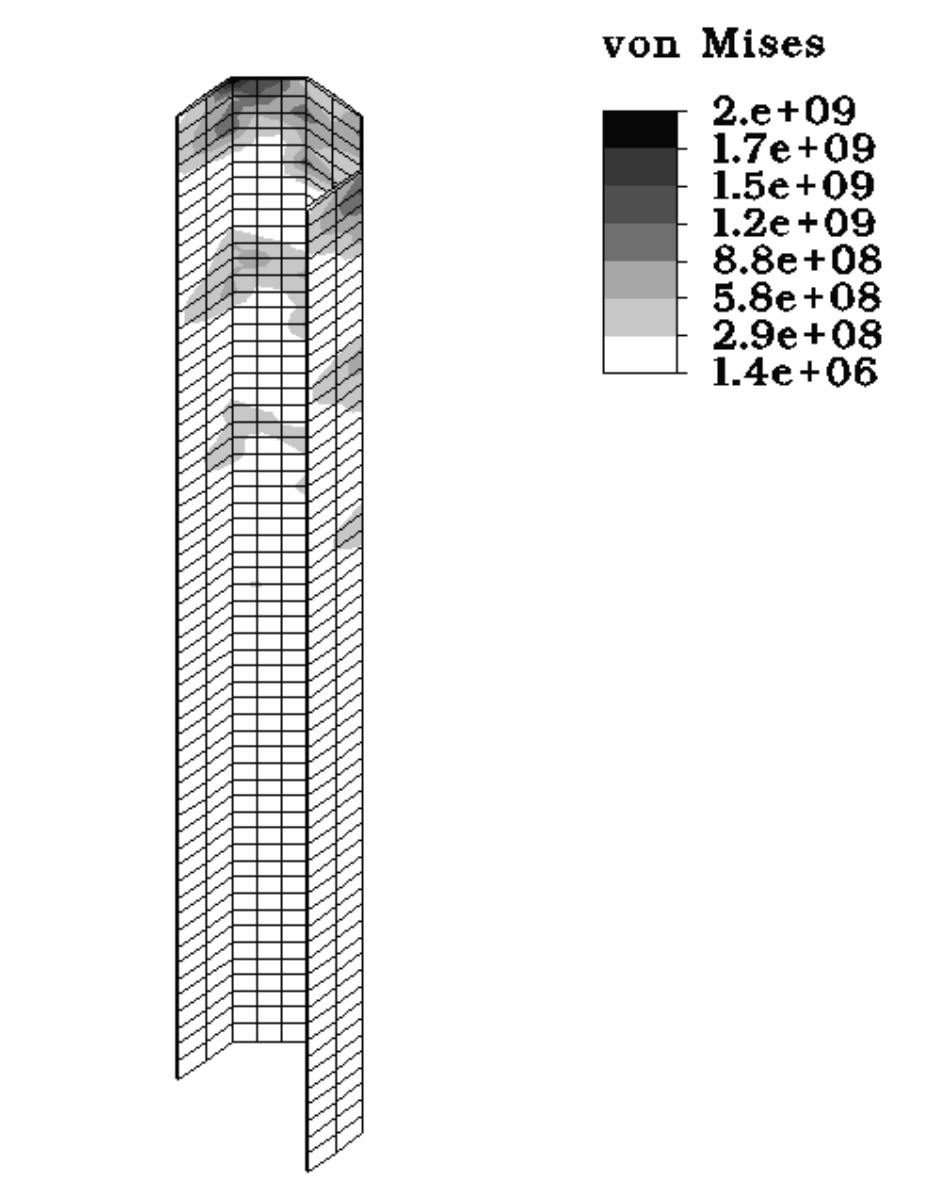

Fig. 3a

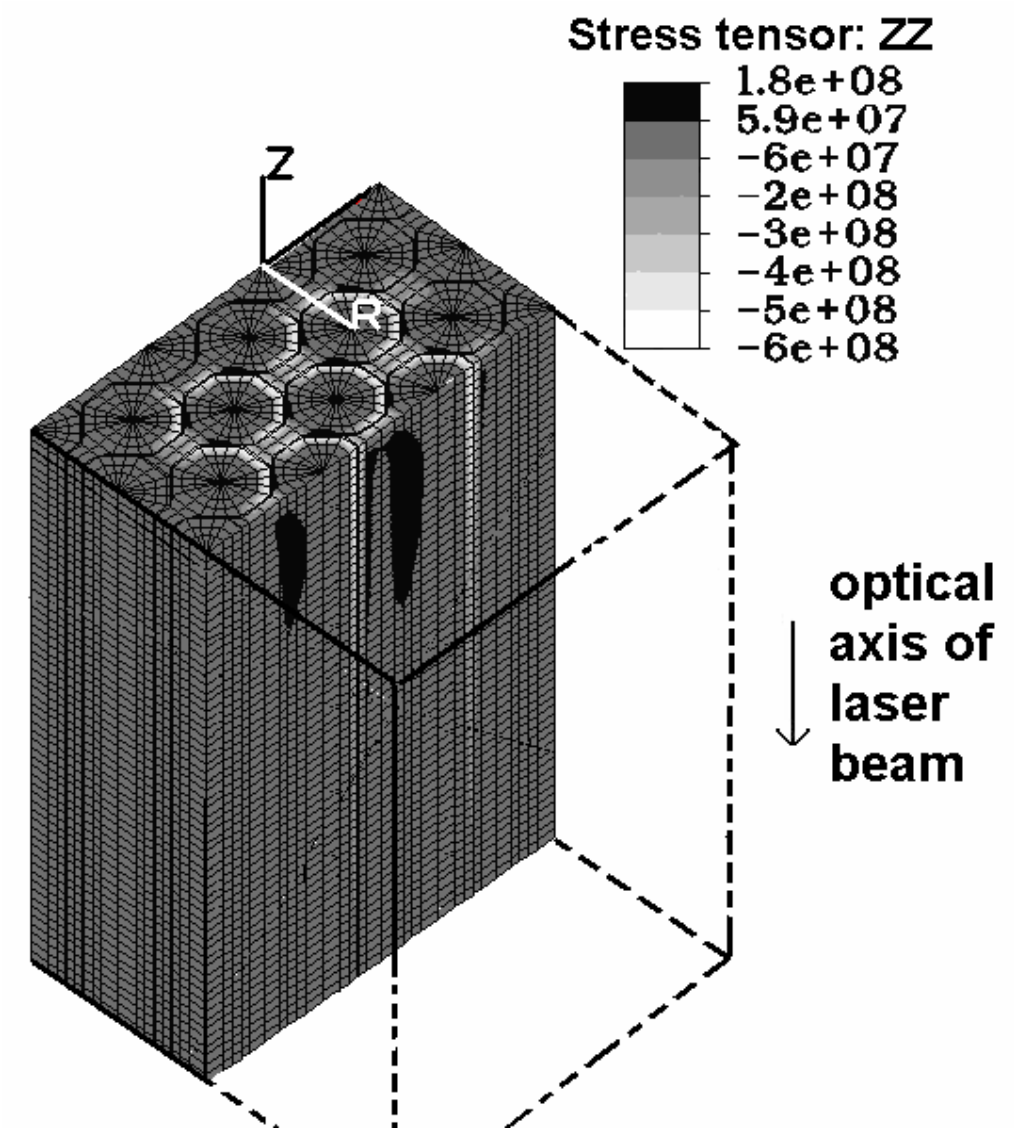
Stress tensor: ZZ
1.8e+08
5.9e+07
-6e+07
-2e+08
-3e+08
-4e+08
-5e+08
-6e+08
Z
R
optical axis of laser beam

Fig. 3b

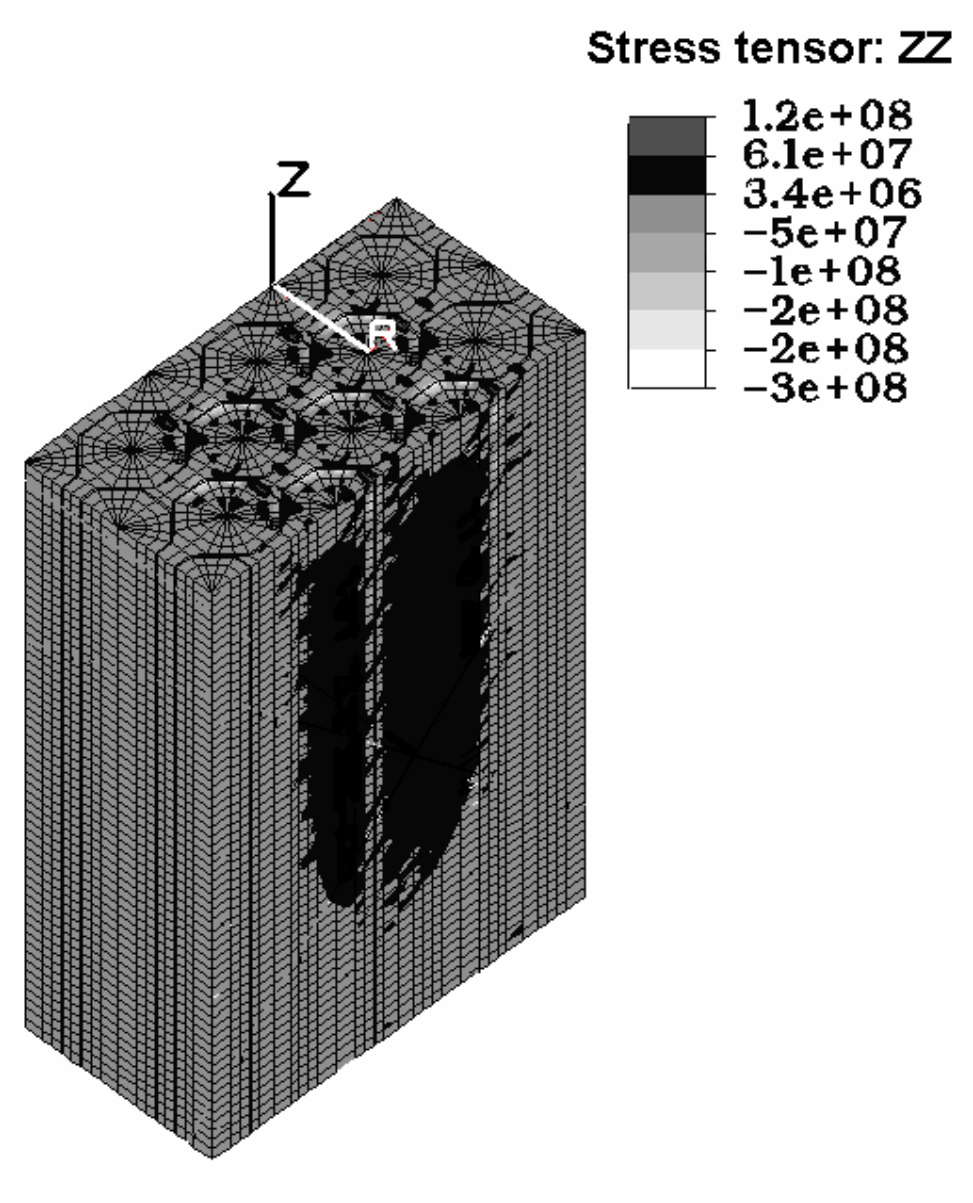
Stress tensor: ZZ
1.2e+08
6.1e+07
3.4e+06
−5e+07
−1e+08
−2e+08
−2e+08
−3e+08
Z
R

Fig. 3c

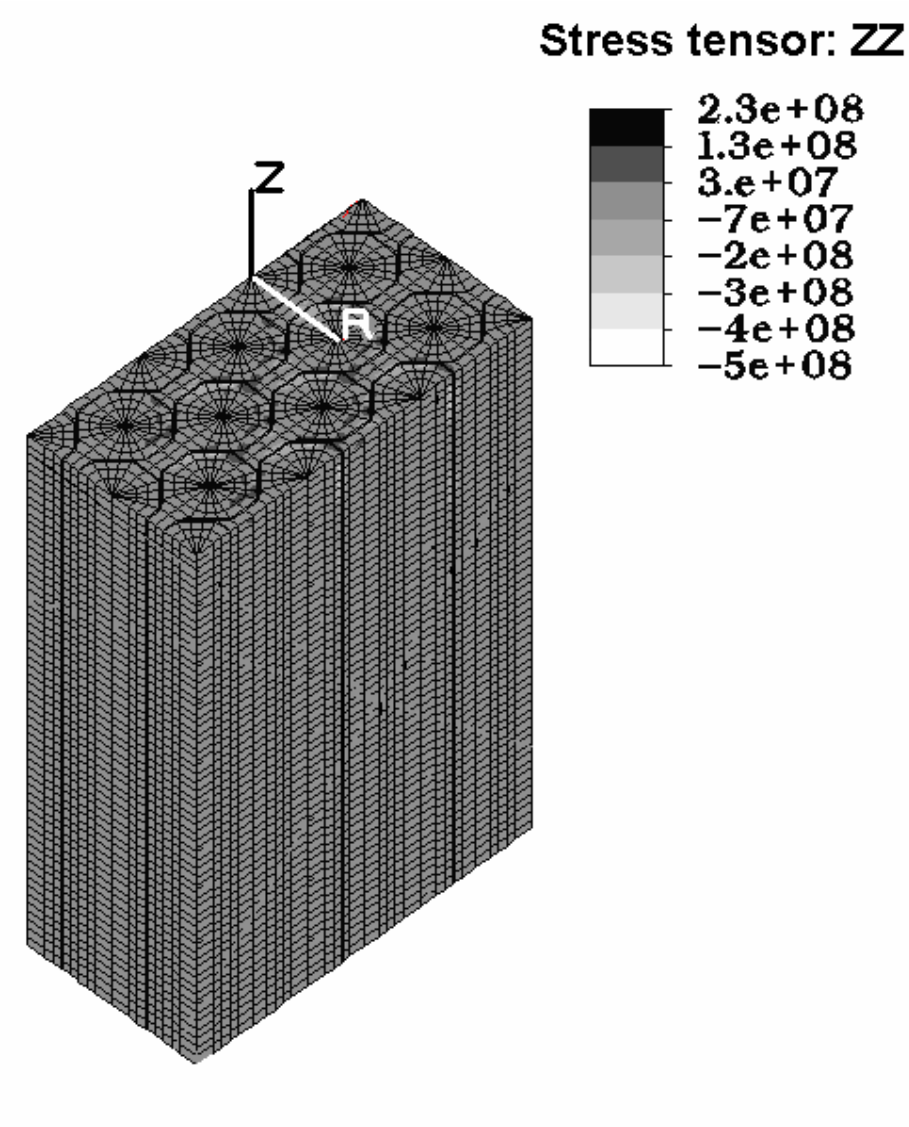
Stress tensor: ZZ
2.3e+08
1.3e+08
3.e+07
−7e+07
−2e+08
−3e+08
−4e+08
−5e+08
Z
R